Applied Catalysis B: Environmental 92 (2009) 333–340

Contents lists available at ScienceDirect

Applied Catalysis B: Environmental

journal homepage: www.elsevier.com/locate/apcatb

Fast catalytic degradation of organic dye with air and MoO_3:Ce nanofibers under room condition

Wei Li [a], Shun Zhao [a], Bin Qi [a], Yang Du [a], Xiaohong Wang [a,*], Mingxin Huo [b,*]

[a] Key Lab of Polyoxometalate Science of Ministry of Education, Faculty of Chemistry, Northeast Normal University, Changchun 130024, PR China
[b] School of Urban and Environmental Sciences, Northeast Normal University, Changchun 130024, PR China

ARTICLE INFO

Article history:
Received 11 February 2009
Received in revised form 2 August 2009
Accepted 7 August 2009
Available online 13 August 2009

Keywords:
Catalytic wet air oxidation
Molybdenum oxide
Cerium oxide
Degradation of dye
Nanofibers

ABSTRACT

One-dimensional Ce doped MoO_3 nanofibers with different Ce doping amount have been synthesized by a combination method of sol–gel process and electrospinning technique. X-ray diffraction (XRD), X-ray photoelectron spectrum (XPS), Fourier transform infrared spectroscopy (FT-IR), scanning electron microscopy (SEM) were used to characterize the resulting samples. These fibers are interesting for a number of catalytic applications. The best catalytic activity was obtained over 11.86 wt.% CeO_2-doped MoO_3 with 98% degradation effect of 0.3 g L^{-1} Safranin-T by air under room condition towards complete degradation products such as HCO_3^- and NO_3^- within 20 min. The leaching test showed that this MoO_3:Ce nanofiber catalyst has an excellent stability and can be used as a rapid heterogeneous catalyst for about ten times by simply treatment.

1. Introduction

Environmental pollution is a serious challenge for the world. Textile dyes and other industrial dyestuffs constitute one of the largest groups of organic compounds containing a large content of aromatics, while conventional biological treatment methods are ineffective for decolorization and degradation in some cases [1]. Therefore, it is urgent to seek available technologies to degrade these organic pollutants. Previous reports have proven that wet air oxidation (WAO) at high temperature and pressure is an effective means for degrading organics and toxic materials in many treatment methods, which exhibits reasonable effectiveness to remove color and chemical oxygen demand (COD) from a dye solution [2]. However, the high pressure (0.5–20 Mp) and high temperature (175–320 °C) are needed [3], which limit the practical application. So it is necessary to study into this process under mild conditions. Catalytic wet air oxidation (CWAO) is recently developed to relax the oxidation condition [4], but it still requires a temperature in the range of 80–180 °C and a pressure in the range of 1–5 MPa [5,6]. From the economical point of view, there is still a need and challenge to improve catalytic activity and long-term stability of heterogeneous catalysts in order to achieve effective degradation of organic compounds at mild condition. By now, there are only a limited number of studies on the CWAO of organic dyes under mild condition [7–10]. These processes used heterogeneous catalysts including mixed metal oxides $CuO/MoO_3/P_2O_5$, $FeO_x/MoO_3/P_2O_5$, mixed metal oxide loading material Fe_2O_3–CeO_2–TiO_2/Al_2O_3, and polyoxometalates $Zn_{1.5}PW_{12}O_{40}$ to achieve the decolorization of organic dyes by air under mild conditions especially under room temperature. So search for a more active and stable heterogeneous catalyst to relax the oxidation condition for WAO is a never-ending task.

In general, both molybdenum oxide and cerium oxide based catalysts have attracted the attention, because of their numerous applications in various fields. Molybdenum oxide based catalysts have been widely used in many important oxide or acid catalytic reactions [11]. Furthermore, cerium oxide (or ceria) based material contains a high concentration of mobile oxygen vacancies, which acts as local sources or sinks for oxygen involved in reactions taking place on its surface. The high oxygen mobility, oxygen storage capacity and strong interaction with the supported metal render this material very interesting for a wide range of catalytic applications involving oxidation and reforming of hydrocarbons [12–14]. Nevertheless, to our knowledge, no work has been reported yet on Ce doping MoO_3 system applied on CWAO of organic dyes. We think if CWAO of dye can occur within very short time at mild condition especially at room temperature and atmospheric pressure, a long existence time of oxygen in the system is needed. Ceria is a well-known additive as an oxygen storage/release capacity, doping some Ce into MoO_3 might enhance the catalytic activity. Therefore, an attempt was made in this present study to shed some light into properties of this

* Corresponding authors. Tel.: +86 431 88930042; fax: +86 431 85099759.
E-mail address: wangxh665@nenu.edu.cn (X. Wang).

0926-3373/$ – see front matter © 2009 Elsevier B.V. All rights reserved.
doi:10.1016/j.apcatb.2009.08.012

catalyst system. And ST, a kind of organic dye was chosen as model target to examine the degradation effect of MoO_3:Ce only using air as oxidant.

In order to obtain a high efficient, high porosity, large surface area, and easy separation, the electrospinning process and the sol–gel process have been used to prepare metal oxide nanofibers. The electrospinning technique has been developed since 1934 for the synthesis of 1D nanomaterials [15]. On the other hand, sol–gel techniques can be employed to prepare precursor solutions, which have been used to deposit coatings by spinning and dipping processes [16]. 1D nanomaterials fabricated by a combination method of sol–gel process and electrospinning have become important for their exceptionally long length, uniform diameter, diverse composition, and high surface, which can be applied in many fields such as catalyst supports [17]. And more importance is that it can make catalytic fiber membranes available for a continuous mode by passing the dye solution through the membrane, which is suitable for the industrial application. So MoO_3:Ce fiber membranes have been prepared by the combination of electrospinning and sol–gel process and evaluated their catalytic activity in degradation of dye by air under mild conditions.

2. Experimental

2.1. Materials

All reagents were of AR grade and used without further purification. Deionized and double-distilled water was used throughout this study. For oxidation degradation, 1.0 g stock solution of dye was prepared in double-distilled water and aqueous solution of needed concentration was prepared from the stock solution. The concentration of dyes' solutions was 0.3 g L^{-1}. The pH of the solutions was adjusted by diluted aqueous solutions of HCl and NaOH.

2.2. Physical measurements

Elemental analysis was carried out using a Leeman Plasma Spec (I) ICP-ES. SEM was operated using XL30 ESEM FEG at 25 kV. XRD patterns of the sample were collected on Japan Rigaku D_{max} 2000 X-ray diffractometer with Cu Kα radiation (λ = 0.154178 nm). XPS were recorded on an Escalab-MK II photoelectronic spectrometer with Al Kα (1200 eV). The clear filtrate solution of the catalytic process was tracked by UV–vis spectroscopy using a 756 CRT UV–vis spectrophotometer. TOC was monitored using a Shimadzu TOC-VCPH total organic carbon analysis system.

2.3. Preparation of MoO_3:Ce nanofibers

Nanofibers of MoO_3:Ce were prepared by a method of sol–gel process and electrospinning technique. $(NH_4)_2Ce(NO_3)_6$ and $(NH_4)_6Mo_7O_{24}{\cdot}4H_2O$ with the molar ratio of 1/0.7, 1/1, 1/1.28 were dissolved in dilute nitric acid and then were mixed with a water–ethanol (v/v 1:4) solution containing citric acid as a chelating agent for the metal ions. The molar ratio of metal ions to citric acid was 1:1. A certain amount of polyvinyl alcohol (PVA) (M_n = 80,000) was added to adjust the viscoelastic behavior of the solution. The solution was stirred for 4 h to obtain a homogeneous hybrid sol for further electrospinning. The as-prepared hybrid precursors were annealed to 600 °C with the heating rate of 2 °C min^{-1} and held there for 5 h in air.

2.4. Catalytic procedure

The stoichiometry of reaction was determined by allowing 0.3 g L^{-1} of dye to be degraded by air at room temperature (25 °C) and atmospheric pressure in the presence of the catalyst. A general procedure was carried out as follows: 0.1 g of MoO_3:Ce catalyst was suspended in a fresh aqueous dye solution (C_0 = 0.3 g L^{-1}, 100 mL) in three-neck glass flask. The air was inputted into the bottom of the suspension with the flowing rate 0.08 m^3/h. This process uses oxygen dissolved in the aqueous solution as an oxidant directly. Oxygen concentration depends on the oxygen solubility at room temperature and atmospheric pressure. 5 mL of samples were taken out by filtration at regular intervals of the experiment. UV–vis spectroscopy was used in the experiment to monitor the degradation of dyes at 524 nm. The removal of dye can be calculated by the following equivalent:

$$Removal\,(\%) = \frac{A_0 - A}{A_0} \times 100\%$$

where A_0 and A are the initial and final absorbance value of dye, respectively.

3. Results and discussion

3.1. Characterization of catalysts MoO_3:Ce nanofibers

From the result of elemental analysis, the contents of the materials are Mo, 53.42%, Ce, 15.50%; Mo, 56.60%, Ce, 11.27%; Mo, 58.60%, Ce, 9.40%, respectively. The final product is denoted as MoO_3:Ce-*x*, where *x* represents Ce loading (wt.%)in the composite. Herein, *x* = 9.54, 11.86, 15.70%, respectively.

The FT-IR spectrum of MoO_3:Ce-11.86 (Fig. 1) showed that three peaks at 996, 864 and 565 cm^{-1} are attributed to Mo–O stretch vibration mode, asymmetric Mo–O bonds and Mo–O–Mo bending vibration mode [18], indicating the existence of MoO_3. In addition, two peaks at 1196, 1385 cm^{-1} are attributed to Ce–O–Ce appeared, showing that CeO_2 existed in the lattice of MoO_3. Due to the decomposition of PVA, $(NH_4)_2Ce(NO_3)_6$ and $(NH_4)_6Mo_7O_{24}{\cdot}4H_2O$, no peaks assigned to ν_{C-H}, ν_{C-C}, ν_{C-O}, ν_{O-H}, ν_{N-H} of PVA, $(NH_4)_2Ce(NO_3)_6$ and $(NH_4)_6Mo_7O_{24}{\cdot}4H_2O$[19] appeared. These results illustrated that Ce doping MoO_3 were obtained when the calcination temperature was above 700 °C. And the bands at 1057 and 1540 cm^{-1} are related to the chemisorbed O_2^- species [20], showing the presence of oxygen adsorbed species (O_2^-) due to the doping of Ce into MoO_3 lattice.

To identify the structure of MoO_3:Ce nanofibers, XRD spectroscopy was performed and the results are given in Fig. 2. It is known that all diffraction peaks can be indexed to those of MoO_3 (JCPDS no. 85-2405), in which the characteristic diffraction peaks of 2θ are at 12.835, 23.670, 25.835, and 39.184°. For doping Ce into MoO_3,

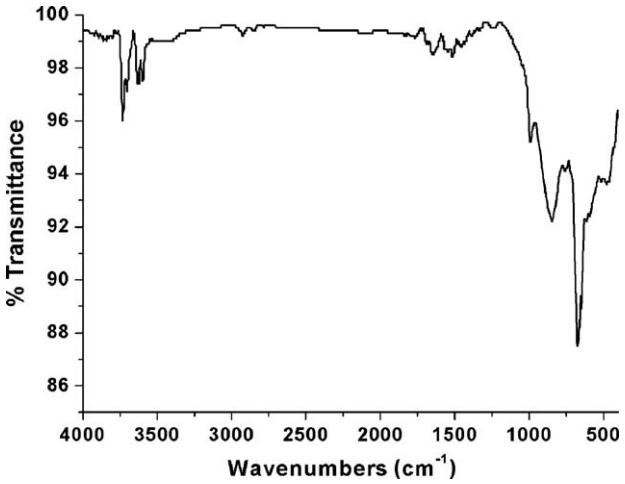

Fig. 1. The IR spectrum of MoO_3:Ce-11.86 nanofibers.

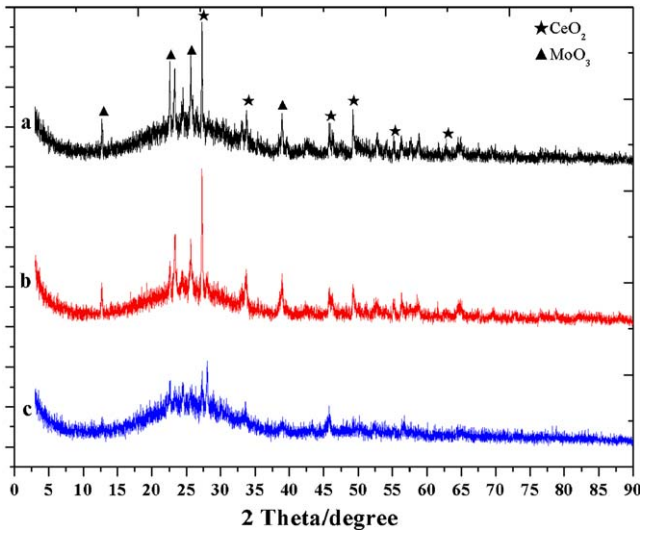

Fig. 2. XRD patterns of (a) MoO_3:Ce-9.54 nanofibers; (b) MoO_3:Ce-11.86 nanofibers; (c) MoO_3:Ce-15.70 nanofibers.

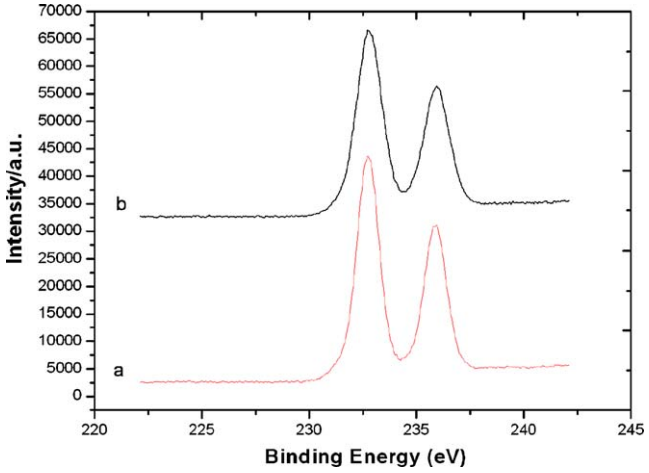

Fig. 3. Binding energy of molybdenum in MoO_3:Ce-11.86 catalyst before reaction (a) and after reaction (b).

there was a litter difference from the JCPDS card of MoO_3 and this phenomenon was observed by Ma [8] in the XRD spectrum of CuO–MoO_3–P_2O_5, which was perhaps due to –Mo–O– bond to –O–Mo–O–, indicating that the valence of molybdenum element in MoO_3:Ce system was +6. As shown in Fig. 2, new reflection peaks appear at $2\theta = 28.56^\circ$ (1 1 1), 32.97° (2 0 0), 47.86° (2 2 0), 56.58° (3 1 1), 59.28° (2 2 2), and 69.48° (4 0 0), corresponding to the Ce (1 1 1), (2 0 0), (2 2 0), (3 1 1) diffraction peaks (JCPDS no. 04-0593), respectively. Obviously, with the increasing of the amount of Ce in MoO_3, all MoO_3 diffraction peaks weakened. There are no peaks attributed to P_2O_5, indicating no phosphorus existence.

The XPS analysis mainly reflects the composition and chemical elementary state of the surface and the inferior surface of sample. In XPS spectrum for Mo 3d of MoO_3:Ce-11.86 (Fig. 3a), the spin–orbit components of the peaks were well defined by two peaks at approximately 235.8 and 232.7 eV, respectively, which indicated that Mo element existed mainly as the chemical state of Mo^{6+} on the nanofibers. And after reaction, the XPS spectrum of Mo 3d (Fig. 3b) kept intact compared to that before the reaction, which indicated that Mo element existed mainly as the chemical state of Mo^{6+} and was constant during the reaction. There is no P 2p at 135 eV, suggesting no phosphorus existence in the MoO_3:Ce nanofibers.

It could be found that the peaks of the Ce 3d (Fig. 4a) were asymmetric and broad. Peak separation method is applied to XPS spectra of Ce 3d and there are four peaks. Both Ce $3d_{5/2}$ and Ce $3d_{2/3}$ levels present five components named respectively V_0, V, V′, V″, V‴ and U_0, U, U′, U″, U‴. According to Burroughs [21], the attribution of the V components ($3d_{5/2}$) is as follows (the same holds for U):

- Cerium(III):V_0, V′: mixture of $4f^2$ O $2p^5$ and $4f^1$ O $2p^6$,
- Cerium(IV):V, VI′: mixture of $4f^2$ O $2p^4$ and $4f^1$ O $2p^5$, V‴: $4f^0$ O $2p^6$.

Therefore it is clear that the cerium exists as the Ce(IV) oxidation state, without any impurity of the Ce(III) oxidation state.

Also it could be found that the peaks of the O 1s (Fig. 4b) were asymmetric and broad. This phenomenon shows that both adsorption oxygen with high binding energy and lattice oxygen with low binding energy existed on the surface of the catalyst. The peak centered at 530.3 eV was associated with the O^{2-} ions in the metal oxide, the peak at 531.4 eV was associated with the O^{2-} ions in the oxygen deficient regions, and the binding energy peak at 533.8 eV was attributed to the loosely bound oxygen such as adsorbed O_2 on the metal oxide's surface.

Fig. 5a shows a typical scanning electron microscopy (SEM) image of the as-prepared MoO_3:Ce-11.86/PVA composite nanofibers with an average diameter of 300 nm. The treated nanofibers in air at 600 °C for 5 h remained as continuous structures (Fig. 5b), and their average diameter was reduced to 200 nm. This size reduction could be accounted to the loss of PVA from the nanofibers and the crystallization of MoO_3.

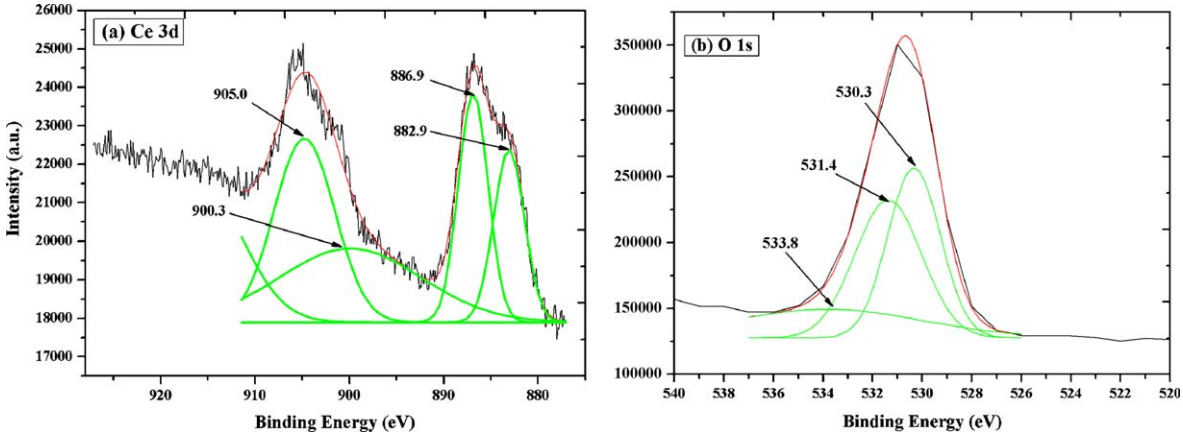

Fig. 4. Binding energy of cerium (a) and oxygen (b) in MoO_3:Ce-11.86 catalyst.

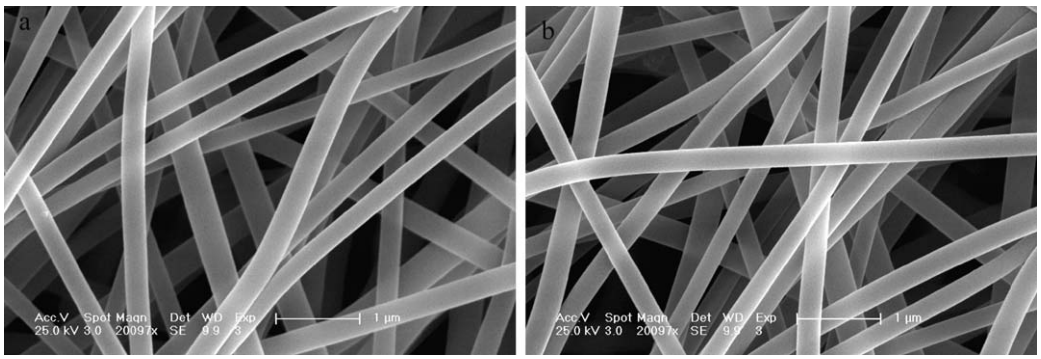

Fig. 5. SEM images of nanofibers. (a) The MoO_3:Ce-11.86/PVA composite nanofibers produced by electrospinning. The average fiber diameter is about 300 nm. (b) The pure MoO_3:Ce-11.86 nanofibers after calcination at 600 °C in air. The average diameter is about 200 nm.

3.2. Catalytic wet oxidation activity of MoO_3:Ce nanofibers

ST (the molecular structure is given in Scheme 1) is selected as the model pollutants because they are well-known textile colorant, which are harmful to human beings. By now, photochemical degradation of the hazardous ST has been carried out [22].

In our previous report [9b], the operational window was $Zn_{1.5}PMo_{12}O_{40}$ nanotube catalyst (1.0 g L^{-1}), air flowing rate 0.08 m^3/h and the dye' concentration 10 mg L^{-1}. We did the catalytic test in the same condition, and it was found that MoO_3:Ce nanofibers can catalyze the decolorization of ST within very short time, i.e. 5 min, showing that MoO_3:Ce nanofibers is more active than $Zn_{1.5}PMo_{12}O_{40}$ nanotube was. It is well known that the dye wastewater with high concentration is very difficult to treat, so we enhanced the concentration of ST from 10 to 300 mg L^{-1} to evaluate the catalytic activity of MoO_3:Ce in order to achieve large-scale utilization. The present tests were operated in suspension (1.0 g L^{-1} catalyst, 100 mL 0.3 g L^{-1} dye) at room temperature and atmospheric pressure with air flowing rate 0.08 m^3/h for 20 min.

3.2.1. Effects of the catalyst

Under above operational window, the degradation effects of ST with different catalysts MoO_3, CeO_2 and MoO_3:Ce-*x* nanofibers are shown in Fig. 6 as a function of time under air at room temperature. It can be seen that without any catalyst and only with flowing air, decolorization efficiency is 4.1% in 20 min and there is no dye being degraded in the beginning of 3 min. This result shows that the oxidation ability of oxygen is limited without catalyst at room temperature. The decolorization of dyes catalyzed by CeO_2 and MoO_3 can reach 21 and 39%, respectively, indicating that these two materials have less catalytic activity in this system under such reaction condition. The catalytic activity is greatly improved by cerium addition. With different doping amounts, the catalytic activity increased firstly then decreased, namely, the catalytic activity range is MoO_3:Ce-9.54 < MoO_3:Ce-15.70 < MoO_3:Ce-11.87. The best activity was obtained when using MoO_3:Ce-11.87 nanofiber as a catalyst, i.e. the decomposition of ST was almost completely in 20 min by flowing air; namely, the color removal percent of ST reached to 98%. Provided that the bleaching reaction follows a pseudo-first-order reaction, the rates of the ST under MoO_3:Ce-*x* nanofibers are estimated to be about 1.26, 1.35, 1.47 mg min^{-1}, respectively. It is assumed that the introduction of cerium into the lattice of MoO_3 increased significantly the mobility of oxygen atoms, therefore the catalytic activity was increased. As a matter of fact, the interaction between MoO_3 and CeO_2 in MoO_3:Ce complex plays a crucial role in the wet air oxidation of dye. This synergistic mechanism can be essentially regarded as a process of oxygen activation, and the oxygen transfer through the redox recycles of Mo^{6+}/Mo^{5+} and Ce^{4+}/Ce^{3+}, which can be proposed as follows:

$$MoO_3 + RH \rightarrow R^{\bullet} + H^+ + Mo_2O_5 \text{ (initiation)} \quad (1)$$

$$Mo_2O_5 + CeO_2 \rightarrow Ce_2O_3 + MoO_3 \quad (2)$$

$$Ce_2O_3 + 1/2O_2 \rightarrow CeO_2 \quad (3)$$

It was suggested that the oxidation of dye (Scheme 2) might occurred on Mo^{6+} sites, which itself was reduced to Mo^{5+}. Reaction (1) occurs on the catalyst surface and it is a fast reaction. The Mo^{5+} was then oxidized to Mo^{6+} by Ce^{4+} (reaction (2)), which itself was reduced to Ce^{3+}. Finally, Ce^{3+} was oxidized to Ce^{4+} by O_2 (reaction (3)). The above redox steps fulfill the catalytic cycle for the CWAO of dye (described as follows), which is usually termed as the Mars-Van Krevelen redox mechanism [23].

Thus, the oxygen transfer from molecular oxygen to active sites of MoO_3 through oxygen reservoir CeO_2 achieved the effective

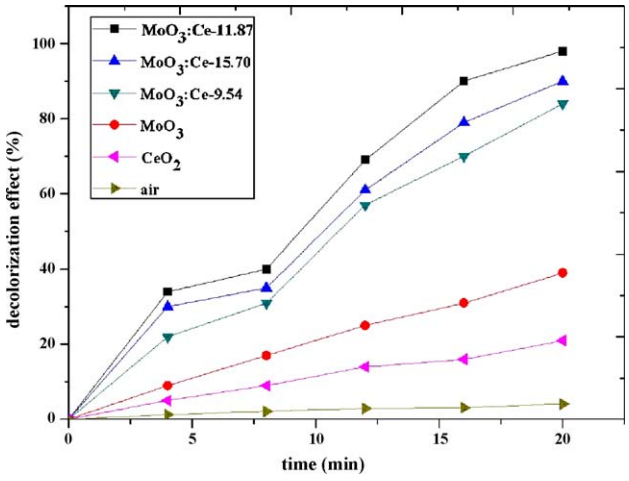

Fig. 6. Decolorization efficiency of dye by different catalysts (1.0 g L^{-1}) at room temperature, 100 mL of 0.3 g L^{-1} dye solution, with the air flowing rate 0.08 m^3/h.

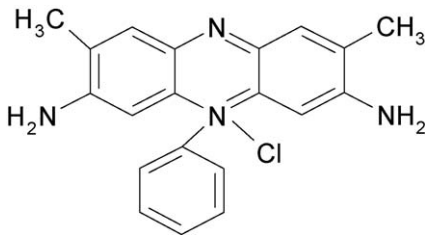

Scheme 1. The structure of ST.

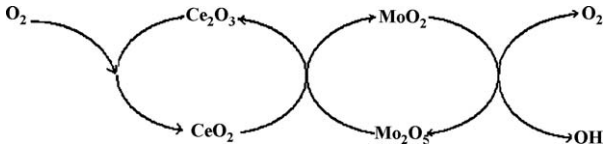

Scheme 2. The possible redox mechanism of MoO_3:Ce in CWAO process.

activity of molecular oxygen. In the meantime, the higher density of molybdenum species as active sites is equally important for the CWAO reaction. So enhancement the doping amount of Ce did not increase the catalytic activity of MoO_3 all the time.

3.2.2. Adsorption capacity of ST on MoO_3:Ce-11.87

It is known that the adsorption capacity on catalyst of dye is a key factor [24], which the more target molecules adsorbed on catalyst, the faster or more complete these molecules decomposed. So the adsorption experiments were carried out to study the adsorption of dyes on MoO_3:Ce-11.87 nanofibers (Fig. 7). Dye solution (C_0 = 0.3 g L^{-1}, 100 mL) was treated in the vacuum reactor in the presence of 0.1 g MoO_3:Ce-11.87 nanofibers, which means that there is no oxygen being introduced into the experimental system. The concentration of dyes decreased sharply and reached maximum ca. 31% in 6 min for ST, suggesting that some adsorption of the reactants onto the catalyst occurred in the beginning of the reaction. However, increasing the stirring time did not decrease the concentration of dyes. This experiment demonstrated that the adsorption of dye by catalyst was not main effect of decolorization of dyes and the true activity came from the catalyst' effect. The adsorption was attributed to the nano-structure of MoO_3:Ce-11.87. It enhanced mass transport for oxygen molecules into and out of the pore structure [25].

The higher activity of MoO_3 nanofibers partially comes from the relatively higher BET surface area (523 m^2 g^{-1}). It can be seen that the microstructure and morphology of the catalyst is one of the important factors for catalytic activity in the decolorization of ST.

In addition, the influence of the temperature on adsorption effect was done (Fig. 7). It can be seen that the adsorption effect increases by increasing temperature from 0 to 35 °C.

The solution pH has great influence on the surface charge of the metal oxide catalyst. Fig. 8 showed the adsorption isotherms of ST on MoO_3:Ce-11.87 catalyst at pH values of 2.97, 5.02, 6.89, 8.93 and 10.51. The adsorption of ST onto the catalyst nanofibers increased as the pH values increased. This phenomenon also observed by

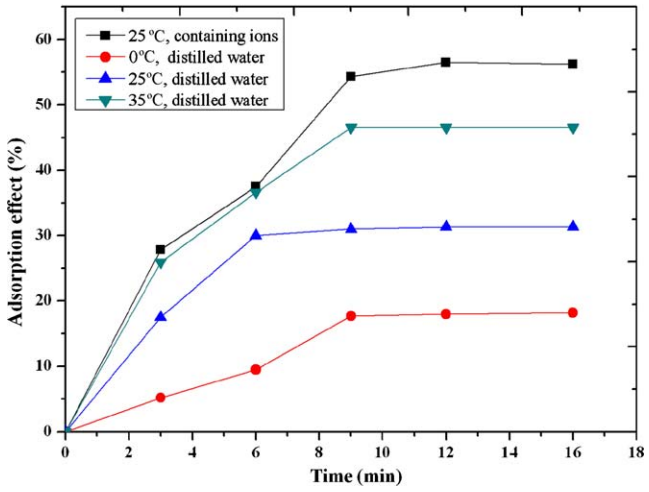

Fig. 7. The adsorption isotherms of dyes on MoO_3:Ce-11.86 nanofibers.

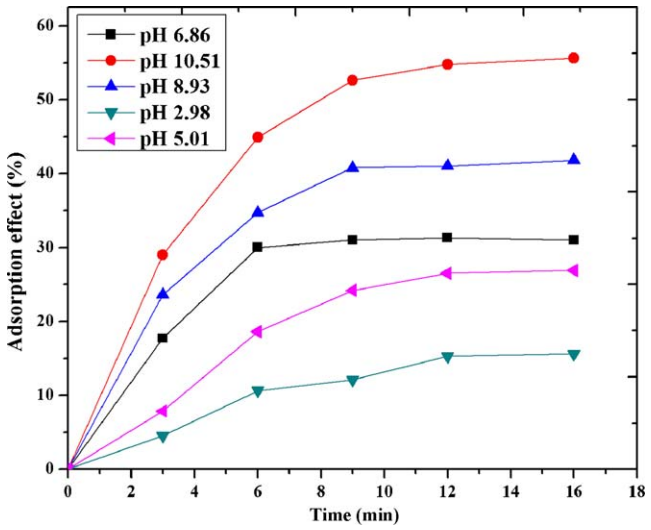

Fig. 8. The adsorption isotherms of dyes on MoO_3:Ce-11.86 nanofibers at different pH.

other MoO_3 catalyst [26]. The points of zero charge of CeO_2 and MoO_3 are pH_{pzc} 6.8 and pH_{pzc} 8.2, respectively. And the number of positively charges on the MoO_3:Ce surface decreases with increasing pH and reaches zero at pH_{pzc}. So since at acidic or weak basic media, the catalyst surface is positively charged and the $Mo–OH_2^+$/$Ce–OH_2^+$ surface repels the dye anions.

From Fig. 7, the adsorption effect decreased in dye solution containing 0.01 M Na_2SO_4 (pH = 6.88). In view of surface charge of MoO_3:Ce, the surface of MoO_3:Ce is occupied by SO_4^{2-}, the positive charges of MoO_3:Ce are reduced and the surface of MoO_3:Ce become less positive, consequently resulting in increasing adsorption of ST on MoO_3:Ce.

3.2.3. Chemical oxygen demand and total organic carbon

Chemical oxygen demand (COD) reflects the extent of contamination by the reductive substances in water. A significant decrease of COD is observed, which the COD removal is about 98%.

Fig. 9 shows TOC reduction as a function of the reaction temperature from 0 to 35 °C. It can be seen that temperature has a significant influence on the dye's mineralization. With the temperature increasing, the TOC reduction of ST increased significantly, while the TOC reduction of ST reached 96.5% at

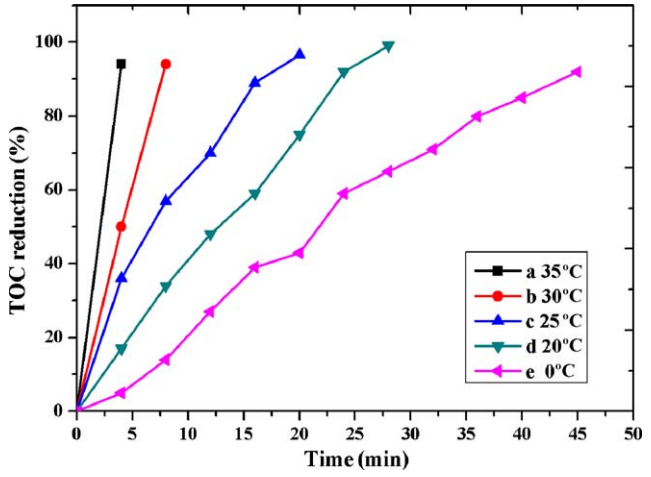

Fig. 9. The TOC reductions of ST at different temperature in the presence of 1.0 g L^{-1} MoO_3:Ce-11.87 catalyst, 100 mL of 0.3 g L^{-1} dye solution with the air flowing rate 0.08 m^3/h.

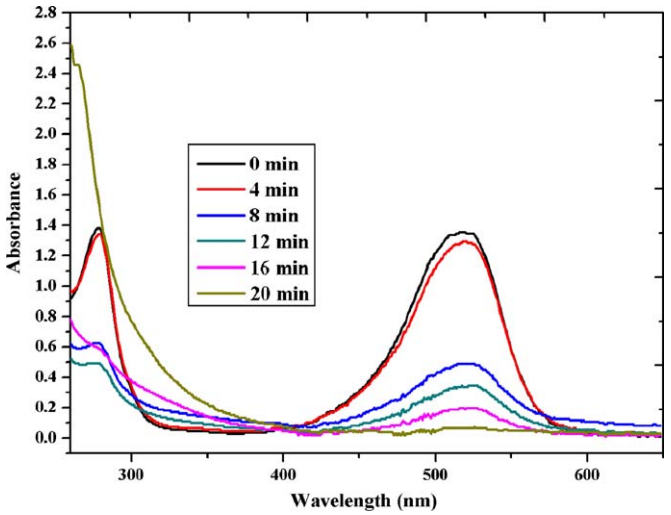

Fig. 10. The UV–vis absorption spectra changes of ST solution.

25 °C and the TOC reductions reached 94% at 35 °C within 4 min. So the temperature can considerably promote the degradation of dyes. We did the degradation experiment at lower temperature such as 0 °C because our city locates at the northeast of China and the temperature is below zero in many months, therefore there is a actual need for wet air oxidation of organic dyes in lower temperature. The TOC reduction reached 92% for about 45 min at 0 °C.

It can be seen from Fig. 10 that two major absorbance peaks at 280 and 524 nm in the initial UV–vis spectra of ST, which are due to benzene ring and 2,3-dihydropyrazine ring [27].

As the treatment time increases, these two peaks become weaker and weaker in intensity until these two peaks totally disappear in 20 min. It indicates that the ST molecules are attacked by $OH^{\bullet}$ radials and the benzene ring and 2,3-dihydropyrazine ring of ST are destroyed into small species.

The typical IR spectra in region 4000–500 cm^{-1} of ST before and after treatment also demonstrated the total mineralization of dye (Fig. 11). The IR spectrum of ST exhibit one aromatic ring C–H stretching vibration peak at 3144 cm^{-1} and three aromatic ring C=C stretching vibration peaks at 1640 and 1493, 1530 cm^{-1}. After treating dye by air for about 20 min, these peaks decrease in intensity to disappear, indicating the total destruction of aromatic ring of dye molecule. In addition, the peaks at 1610 and 1331 cm^{-1} are due to the –N=C– bond and the C–N stretching band of dyes molecules, respectively. The disappearance of these two peaks associates with destruction of 2,3-dihydropyrazine structure and C–N bond of Ar–NH_2. Moreover, the appearance of new peaks for ST at 1590, 926 and 896 cm^{-1} may be attributed to C–O vibration of HCO_3^- anion. And the new peak for ST at 1380 cm^{-1} is due to N–O vibration of NO_3^- anion. There is no Cl^- vibrational peak in the IR spectra because ST is ionic molecule and chlorine exists as Cl^- anion, so $AgNO_3$ is used to detect Cl^- in the final dye, which shows some amount of Cl^- existence in the final dye solution. As a result, catalyzed by MoO_3:Ce nanofibers, the organic dyes are oxidized by air and subsequently degraded into small inorganic species such as HCO_3^-, Cl^- and NO_3^- anions. The organic dyes are totally mineralized as TOC results and this catalyst is available to apply in dye's degradation.

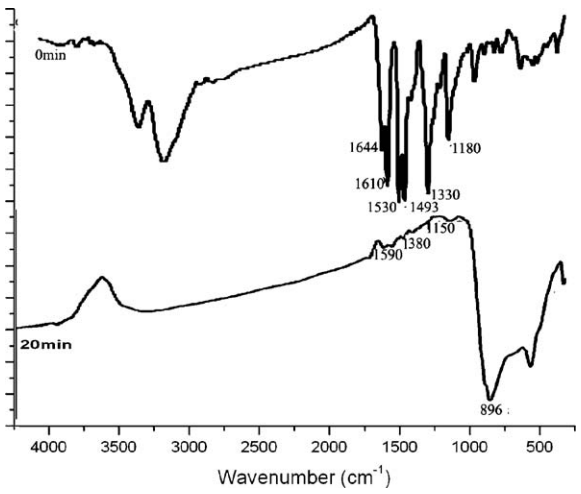

Fig. 11. Change of ST in FT-IR spectra during degradation.

3.2.4. Separation and recovery of the catalyst

The life span of catalyst is a more important parameter for the evaluation of a catalyst. After the reaction finished, the catalyst MoO_3:Ce-11.87 nanofibers was flowing upon the suspensions, which was easily to be separated. The nanofibers were washed by ethanol to remove the dye which absorbed onto the surface of the catalyst and reused. Ethanol was distilled to be reused, and the catalyst decanted for collection. The amount of Mo determined by ICP-AES in the resulting clear solution was 2.7% during ten times, which confirmed the less solubility of the catalyst during the reaction process. The catalyst was thoroughly washed with ethanol and water alternatively in order to remove the dye compound which was attached onto the catalyst surface, then the catalyst would be reused in the next catalytic experiment. Compared with the survey of fresh catalyst (Fig. 12a), the bonding energies of Mo 3p, Ce 3d does not shift after the reaction (Fig. 12b), which means that the oxidation states of Mo and Ce did not change and this catalyst is stable during the reaction and the dye adsorbing on the surface of the nanofibers can be easily removed by simple washed with ethanol. The catalytic activity of the degradation of ST was maintained efficiently after ten repeated experiments with slightly decrease (Fig. 13).

3.3. Degradation mechanism

In order to determine the main active species responsible for the degradation of dye molecules, comparison experiments of

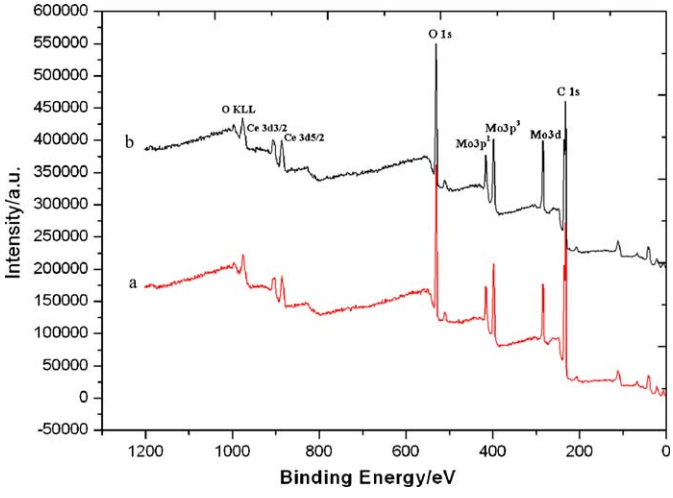

Fig. 12. Survey XPS spectra of MoO_3:Ce-11.86 nanofibers catalyst before (a) and after the reaction (b).

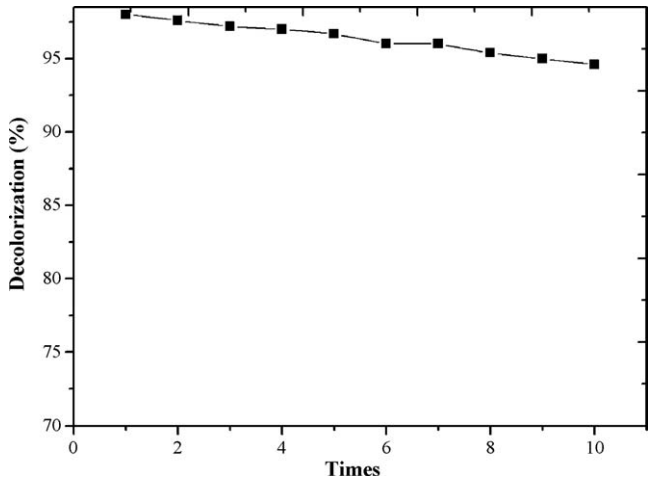

Fig. 13. Cycling runs in the decolorization of ST in the presence of MoO_3:Ce-11.86 nanofibers catalyst, 100 mL of 0.3 g L^{-1} dye solution, with the air flowing rate 0.08 m^3/h.

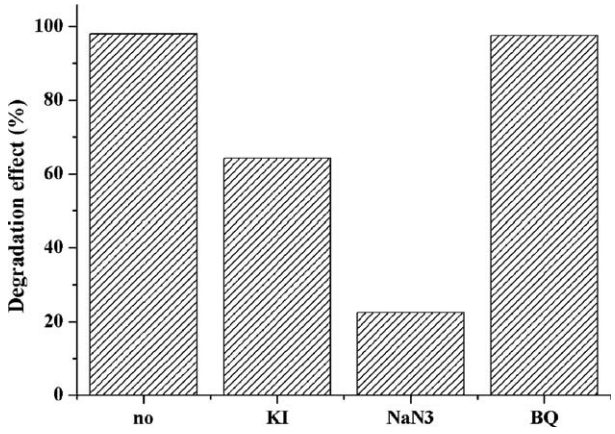

Fig. 14. Effects of scavenging agents on degradation of ST in the presence of 2 mM of 1,4-benzoquinone (BQ), NaN_3 and KI. Other experimental conditions same as Fig. 6.

scavenger-loaded condition were undertaken (Fig. 14). The formation of possible oxidative intermediate species, such as singlet oxygen ($^1O_2$), superoxide ($O_2^{\bullet-}$), and hydroperoxy ($HO_2^{\bullet}$), or hydroxyl radical ($OH^{\bullet}$) if it exists, under WAO conditions has been investigated indirectly, with the use of appropriate quenchers of these species. In this type of experiments, a comparison is made between the original decolorization curves of ST/MoO_3:Ce-11.86 dispersions with those obtained after addition of millimolar concentrations of quenchers in the initial solution, under otherwise identical conditions. In Fig. 14, trace a is the decolorization curve without any quenchers and b, c, d are respective for addition of KI (a quencher of $OH^{\bullet}$ radical on catalyst surface [28]), sodium azide (NaN_3, a singlet oxygen quencher [29] but may also interact with $OH^{\bullet}$ radical [30]) and 1,4-benzoquinone ($C_6H_4O_2$, BQ, a quencher of superoxide radical [31]). It is observed that NaN_3 and KI affected the degradation rate of ST throughout the experiment. This result indicates that $^1O_2$ or $OH^{\bullet}$ is the active oxidative species involved in this CWAO system. The effect of NaN_3 is higher than that of KI, showing that besides of $OH^{\bullet}$, single oxygen $^1O_2$ was formed as possible oxidative intermediate species during the reaction. In addition, BQ did not affect the degradation rate of ST, showing $O_2^{\bullet-}$ was not the oxidative intermediate species. The above results demonstrated that the reaction takes place through a radical and single oxygen mechanism.

4. Conclusion

A present study reported the synthesis of MoO_3:Ce nanofibers prepared by a combination method of sol–gel process and electrospinning technique and employment as a catalyst for CWAO of ST at mild conditions. When treating high concentration dyes (0.3 g L^{-1}), MoO_3:Ce-11.86 nanofibers exhibits an excellent catalytic activity in the CWAO process under such a mild room condition, while ST molecules are completely mineralized into small inorganic species during a very short time, i.e. 20 min at room temperature and 45 min at 0 °C. The higher catalytic activity of MoO_3:Ce-11.86 nanofibers comes from the synergistic effect between MoO_3 and Ce, that is increase of the mobility of oxygen atoms by the introduction of cerium into the lattice of MoO_3, the interaction between MoO_3 and CeO_2. In addition, nanofiber structure with high surface area exhibits some positive effect on the catalytic activity. Moreover, this MoO_3:Ce-11.86 nanofiber is insoluble in water and stable during ten reused times simply washed with ethanol. This catalytic process is a commercial and green chemical pathway which exhibits potential industrial application in dye degradation. And the studies on the treatment of actual dye using a continuous mode are undergoing.

Acknowledgements

Supported by the National Natural Science Foundation of China (No. 20871026), analysis and testing foundation of Northeast Normal University, the Science Foundation for Young Teachers of Northeast Normal University (No. 20080302).

References

[1] X.W. Zhang, Y.Z. Wang, G.T. Li, J.H. Qu, J. Hazard. Mater. 134 (2006) 181–186.
[2] D.M. Sonnen, R.S. Reiner, I.A. Weinstock, Ind. Eng. Chem. Res. 36 (1998) 4134–4142.
[3] G. Neri, A. Pistone, C. Milone, S. Galvagno, Appl. Catal. B: Environ. 38 (2002) 321–329.
[4] D.K. Lee, I.C. Cho, G.S. Lee, S.C. Kim, D.S. Kim, Y.K. Yang, Sep. Purif. Technol. 34 (2004) 43–50.
[5] S.C. Kim, D.K. Lee, Catal. Today 97 (2004) 153–158.
[6] J. Guo, M. Al-Dahhan, Chem. Eng. Sci. 60 (2005) 735–746.
[7] Y. Liu, D.Z. Sun, Appl. Catal. B: Environ. 72 (2007) 205–211.
[8] H.Z. Ma, Q.F. Zhuo, B. Wang, Environ. Sci. Technol. 41 (2007) 7491–7496.
[9] (a) F. Chai, L.J. Wang, L.L. Xu, X.H. Wang, J.G. Huang, Dyes Pigments 76 (2008) 113–117;
(b) Y. Zhang, D.L. Li, Y. Chen, X.H. Wang, S.T. Wang, Appl. Catal. B: Environ. 86 (2009) 182–189.
[10] Q.F. Zhuo, H.Z. Ma, B. Wang, F. Fan, J. Hazard. Mater. 153 (2008) 44–51.
[11] J. Haber, The Role of Molybdenum in Catalysis, Climax Molybdenum Co., Ann Arbor, MI, 1981.
[12] A. Trovarelli, Catal. Rev. Sci. Eng. 38 (1996) 439–520.
[13] N. Al-Yassir, R.L.V. Mao, Appl. Catal. A: Gen. 332 (2007) 273–288.
[14] V.S. Mishra, V.V. Mahajani, J.B. Joshi, Ind. Eng. Chem. Res. 34 (1995) 2–48.
[15] A. Formhals, U.S. Pat. Specif. 1 (1934) 504–975.
[16] J.W. Zhai, L.Y. Zhang, X. Yao, S.N.B. Hodgson, Surf. Coat. Technol. 138 (2001) 135–140.
[17] E. Formo, E. Lee, D. Campbell, Y.N. Xia, Nano Letters 8 (2008) 668–672.
[18] T.S. Sian, G.B. Reddy, Appl. Surf. Sci. 236 (2004) 1–5.
[19] S.Z. Li, C.L. Shao, Y.C. Liu, S.S. Tang, R.X. Mu, J. Phys. Chem. Solids 67 (2006) 1869–1872.
[20] L. Kundakovic, M. Flytzani-Stephanopoulos, Appl. Catal. A 171 (1998) 13–29.
[21] P. Burroughs, A. Hammett, A.F. Orchard, G. Thornton, J. Chem. Soc., Dalton Trans. (1976) 1686–1698.
[22] (a) V.K. Gupta, R. Jain, A. Mittal, M. Mathur, S. Sikarwar, J. Colloid Interface Sci. 309 (2007) 464–469;
(a) J.J. Li, S.Q. Liu, Y.Y. He, J.Q. Wang, Micropor. Mesopor. Mater. 115 (2008) 416–425.
[23] K.T. Ranjit, I. Willner, S.H. Bossmann, A.M. Braun, Environ. Sci. Technol. 35 (2001) 1544–1549.
[24] M.W. Xue, X.D. Gu, J.P. Chen, H.L. Zhang, J.Y. Shen, Thermochim. Acta 434 (2005) 50–54.

[25] Y. Yang, Q.Y. Wu, Y.H. Guo, C.W. Hu, E.B. Wang, Mol. J. Catal. A: Chem. 225 (2005) 203–212.
[26] C. Karunakaran, R. Dhanalakshmi, Solar Energy Mater. Solar Cells 92 (2008) 1315–1321.
[27] F. Wu, N.S. Deng, H.L. Hua, Chemosphere 41 (2000) 1233–1238.
[28] S.H. Yoon, J.H. Lee, Environ. Sci. Technol. 39 (2005) 9695–9701.
[29] C. Schweitzer, R. Schmidt, Chem. Rev. 103 (2003) 1685–1757.
[30] E. Frati, A.M. Khatib, P. Front, A. Panasyuk, F. Aprile, D.R. Mitrovic, Free Radic. Biol. Med. 22 (1997) 1139–1144.
[31] J. Bandara, J. Kiwi, New J. Chem. 23 (1999) 717–724.